Graphene/carbon fibers decorated with V-doped titanium oxide: an efficient visible-light driven photocatalyst

Z. G. Li[a,b,*], B. Zeng[a]
[a]*College of Mechanical Engineering, Hunan University of Arts and Science, Changde 415000, People's Republic of China*
[b]*Hunan Collaborative innovation Center for construction and development of Dongting Lake Ecological Economic Zone*

The graphene/carbon hybrid nanofibers decorated with vanadium-doped TiO_2 nanoparticles (G/CF/V-TiO_2) were successfully prepared by electrospinning technique and carbonization. The product was characterized by scanning and transmission electron microscopy, X-ray diffractometry, ultraviolet-visible diffuse reflectance spectroscopy, and photoluminescence spectroscopy. Results showed that the graphene/carbon nanofibers had a continuous fiber structure with uniform distribution of V-TiO_2 nanoparticles on their surface. In the photodegradation of methylene blue (MB), G/CF/V-TiO_2 showed a significant increase in the reaction rate under visible light. The enhanced photocatalytic activity could be ascribed to the doping of V into TiO_2 and the carbon-based photocatalytic system, which resulted in an effective visible light response and a rapid separation of photoinduced electron-hole pairs. The strategy presented here can be adopted for synthesizing highly efficient visible-light-driven photocatalysts.

Received February 19, 2021; Accepted June 15, 2021)

Keywords: Graphene, Carbon fibers, Photocatalytic

1. Introduction

In recent years, TiO_2 has been widely investigated for its applications in cleaning up of environment[1]. However, its photocatalytic performance suffers due to low absorption (UV region only) and high charge carrier recombination[2]. Therefore, effective utilization of visible light and improving the separation of photo generated electron-hole pairs are the two important features of TiO_2-based photocatalysts.

Incorporation of metal ions into the TiO_2 crystal lattice can narrow the bandgap and extend its light absorption in the visible region[3]. Thus, various dopants, such as Cr, Mo, Fe, etc., have been extensively investigated[4]. Among the various dopants tested, doping of V in TiO_2 was found to be attractive, since it could move the Fermi energy level towards the bottom of CB and adjusts the narrowed band gap, which could significant extend the light absorption in the visible light region[5].

In addition, anchoring of TiO_2 to carbon-based substrates, such as carbon fiber[6], graphene[7], and activated carbon[8], is an effective way for promoting the separation of photo -generated electron-hole pairs. Owing to their large surface area, good conductivity, and good flexibility, carbon fibers have high potential applications in the photocatalytic field. Particularly, nanofibers with one-dimensional (1D) conducting pathways facilitate the transfer of electrons to achieve maximum photocatalytic performance[9-10]. Recently, combination of carbon fibers with TiO_2 has been extensively investigated. For example, Byeong grew TiO_2 nanoparticles on the surface of activated carbon fibers by a hydrothermal process. This nanocomposite showed high photocatalytic oxidation of benzene, due to the minimization of electron-hole recombination[11]. Therefore, the synthesis of carbon fiber/TiO_2 composites and their applications as a catalyst, become important.

The formation of a hybrid by the combination of carbon fibers and graphene nanosheets with metal oxides shows synergetic effects and multifunctional properties, which make the

* Corresponding author: 676747495@qq.com

photocatalytic activity superior. Recently, many efforts have been devoted to the fabrication of carbon fibers/graphene/TiO_2 hybrids. For example, Kim synthesized graphene/carbon composite nanofibers attached with TiO_2 nanoparticles, which showed significant increase in the degradation for MB under visible light[12]. Therefore, the synthesis of carbon fiber/graphene-TiO_2 has great potential applications in photocatalysis.

Considering all the aspects discussed above, our study reports the fabrication of graphene/carbon fibers/V-doped TiO_2 composites using electrospinning method, which exhibited improved photocatalytic efficiency in the visible spectrum. As expected, V doped TiO_2 could enhance the light absorption in visible region and graphene/carbon fibers acted as electron acceptor to facilitate the separation of the photogenerated electron-hole pairs.

2. Experimental details

2.1. Synthesis of G/CF/V-TiO_2.

Typically, polyacrylonitrile (2 g, PAN, >99% purity, Aladdin), graphene (0.1 g), titanium dioxide (0.5 g, TiO_2, >99% purity, Aladdin), and acetylacetone vanadium (0.01g, $V(C_5H_7O_2)_3$, >98% purity, Aladdin) were added to 12 mL of *N*, *N*-dimethylformamide (DMF, >99.8% purity, Macklin) and stirred for 4 h. The solution was electrospun at a voltage of 20 kV and feed rate of 0.01 $mm \cdot s^{-1}$. The as-prepared product was then placed in an autoclave and heated at 650 °C for 6 h under N_2 atmosphere. For comparison, G/CF/TiO_2 was prepared by the same method, but without adding $V(C_5H_7O_2)_3$. V-TiO_2 was obtained by heating TiO_2 (0.5 g) and $V(C_5H_7O_2)_3$ (0.01 g) at 650 °C for 6 h under N_2 atmosphere.

2.2. Characterization

The morphology was studied by transmission electron microscopy (TEM, JEOL JEM-2100F) and scanning electron microscopy (SEM, Hitachi S4800). The phases were characterized by X-ray diffractometry (XRD, Bruker D2 PHASER). UV-vis diffuse reflectance spectral analysis was conducted on a UV-Vis spectrophotometer (UV-2550, Shimadzu) and photoluminescence spectra were collected using a spectrometer (IHR550, Horiba) at an excitation wavelength of 345 nm.

2.3. Photocatalytic experiment

In a typical experiment, the photocatalyst (0.05 g) was mixed with 300 mL of methylene blue solution (MB, 10 $mg.L^{-1}$) and transferred to a cylindrical reactor (0.5 L). The reactor was kept in a dark place and after it reached desorption/adsorption equilibrium, a 500 W Xe lamp with a cut filter was irradiated. Aliquots of MB solution (5 mL) were withdrawn at 20 min intervals for measurement of absorption. The degradation was calculated using the equation $[1-(C_e/C_0)]/100\%$, where C_0 is absorbance of initial MB solution (before light irradiation) and C_e is absorbance of MB solution after irradiation for a specific time period.

3. Results and discussion

Fig. 1a showed the XRD spectrum of G/CF/V-TiO_2. The peaks at 25.3°, 37.8°, 48.0°, 53.9°, 62.7°, 70.3°, and 75.0° could be attributed to (101), (004), (200), (105), (204), (213), and (215) crystal planes of anatase form of TiO_2 (JCPDS card 21-1271)[13]. The typical peaks of graphene/carbon fibers could not be detected, probably due to the overlapping of peaks at 25.0° for graphene/carbon fibers with the (101) peak of TiO_2[14].

UV-vis diffuse reflectance spectra of the samples were presented in Fig. 1b. The spectra for absorption edges of G/CF/V-TiO_2 and V-TiO_2 showed obvious red shifting compared to that of pure TiO_2. Similarly, absorption in the visible-light regions for G/CF/V-TiO_2 and V-TiO_2 showed tremendous increase as compared to pure TiO_2. Particularly, G/CF/V-TiO_2 showed maximum red shift and the strongest light absorption in the visible-light regions of the three samples. This could be attributed to the doping of V and incorporation of G/CF[15]. Thus, the widening of utility range of visible light in turn considerably increased the photocatalytic activity of G/CF/V-TiO_2 under visible-light irradiation.

Photoluminescence study helped to evaluate the efficiency of charge carrier separation in the semiconductor. Fig. 1c showed that the PL emission spectra of three samples were centered at around 468 nm and the emission peak of G/CF/V-TiO_2 was the weakest. The low emission peak implied an increase in transfer of photoinduced electrons in the composites. This was due to effective electron trap levels after V doping and channels for transport of conductive electrons between the carbon scaffolds with diameters of about 100-200 nm and TiO_2[16].

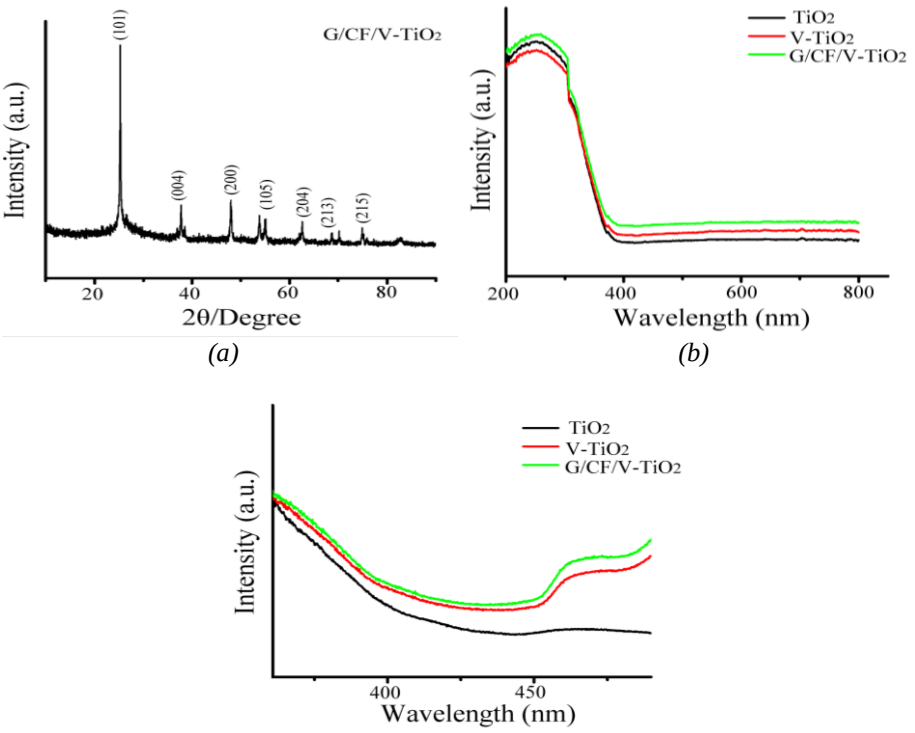

Fig. 1. (a) XRD, (b) UV/Vis diffuse reflectance spectra, (c) photocurrent response spectra of the samples.

The TEM image in Fig. 2b showed a large number of nanoparticles with particle sizes of 10-20 nm that had successfully grown on the surface of the G/CF along with the distinctly visible wrinkled graphene sheet (shown using arrows in the inset of Fig. 2b).

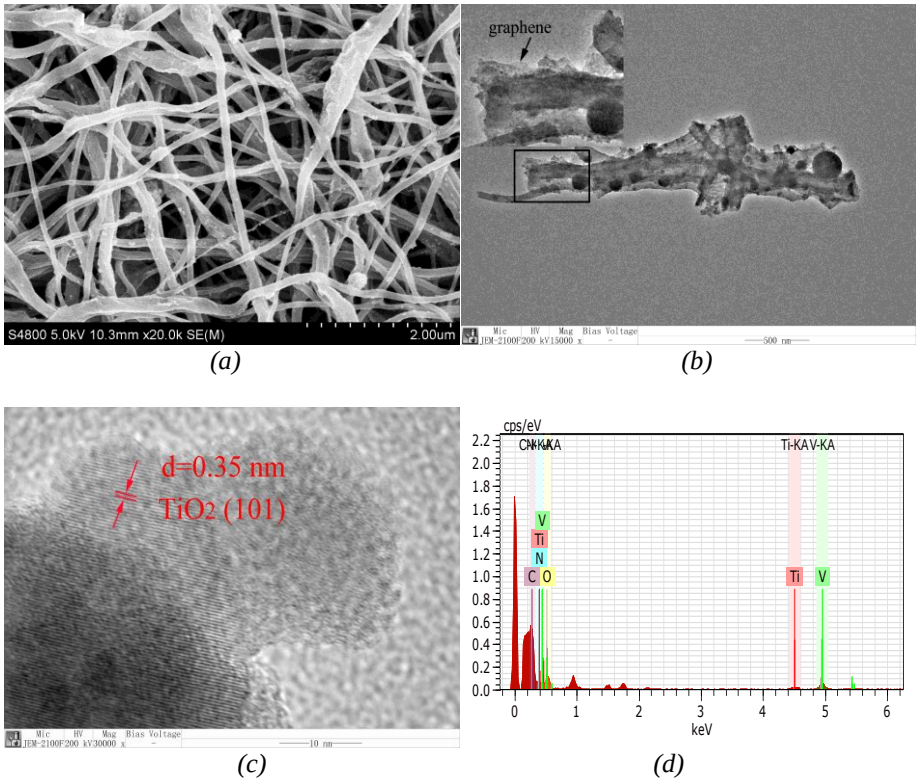

Fig. 2. (a)SEM, (b)TEM, (c)HRTEM, (d) EDS image of G/CF/V-TiO_2.

The interlayer distance planes as measured from high-resolution TEM image in Fig. 2c was found to be 0.35 nm, which was very close to that of (101) plane of TiO_2 (JCPDS 48-1719)[17]. Energy-dispersive spectra (EDS) in Fig. 2d proved that Ti, O, V, and C were present in the composite and this confirmed the formation of the composites of V-doped TiO_2 decorated graphene/carbon nanofibers.

Fig. 3 showed the TEM image and EDS mapping of G/CF/V-TiO_2 sample. In Fig. 3a, the TEM image of the composite showed fibrous nature and the EDS profiles (Fig. 3b) of C were similar to that of fiber structure. Figs. 3c and d showed the presence of Ti and O elements and it was also evident that the graphene/carbon fibers were fully, uniformly, and compactly covered with TiO_2 nanoparticles. Moreover, the homogeneous distribution of V element in the composites (as shown in Fig. 3e) revealed that V elements were doped into the lattices of TiO_2. All these results confirmed that the graphene/carbon fibers were firmly coated with V-doped TiO_2 nanoparticles.

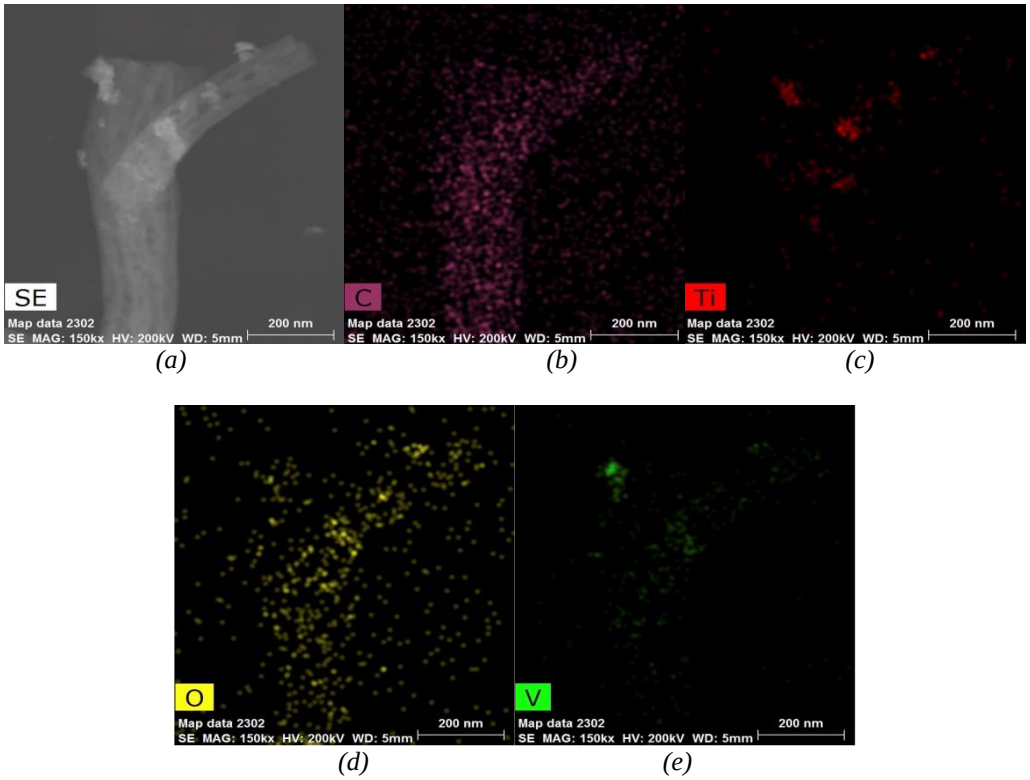

Fig. 3. (a) TEM of EDS mapping of selected area, (b) element C mapping, (c) element Ti mapping, (d) element O mapping, (e) element V mapping of G/CF/V-TiO_2.

The elemental composition of G/CF/V-TiO_2 was further analyzed by XPS analysis. The survey spectrum indicated the presence of Ti, O, C, and V elements (Fig. 4a). The high-resolution Ti 2p spectrum (Fig. 4b) showed two main peaks with binding energies of 458.98 (Ti 2p3/2) and 464.88 eV (Ti 2p1/2)[18]. The O 1s spectrum showed peak at binding energy of 530.04 eV, which corresponded to Ti-O bonding[18]. The C 1s spectrum (Fig. 4d) showed a peak at 284.68 eV, which was attributed to the C-C bond[19]. The high-resolution XPS spectrum of V 2p in Fig. 4e showed three main peaks with binding energies of 516.88 (V^{4+}, 2p3/2), 517.43 (V^{5+}, 2p3/2), and 524.78 eV (V^{5+}, 2p 1/2)[20]. These peaks indicated the successful incorporation of V dopant into the host TiO_2 structure with the formation of new valence states, V^{4+}/V^{5+}.

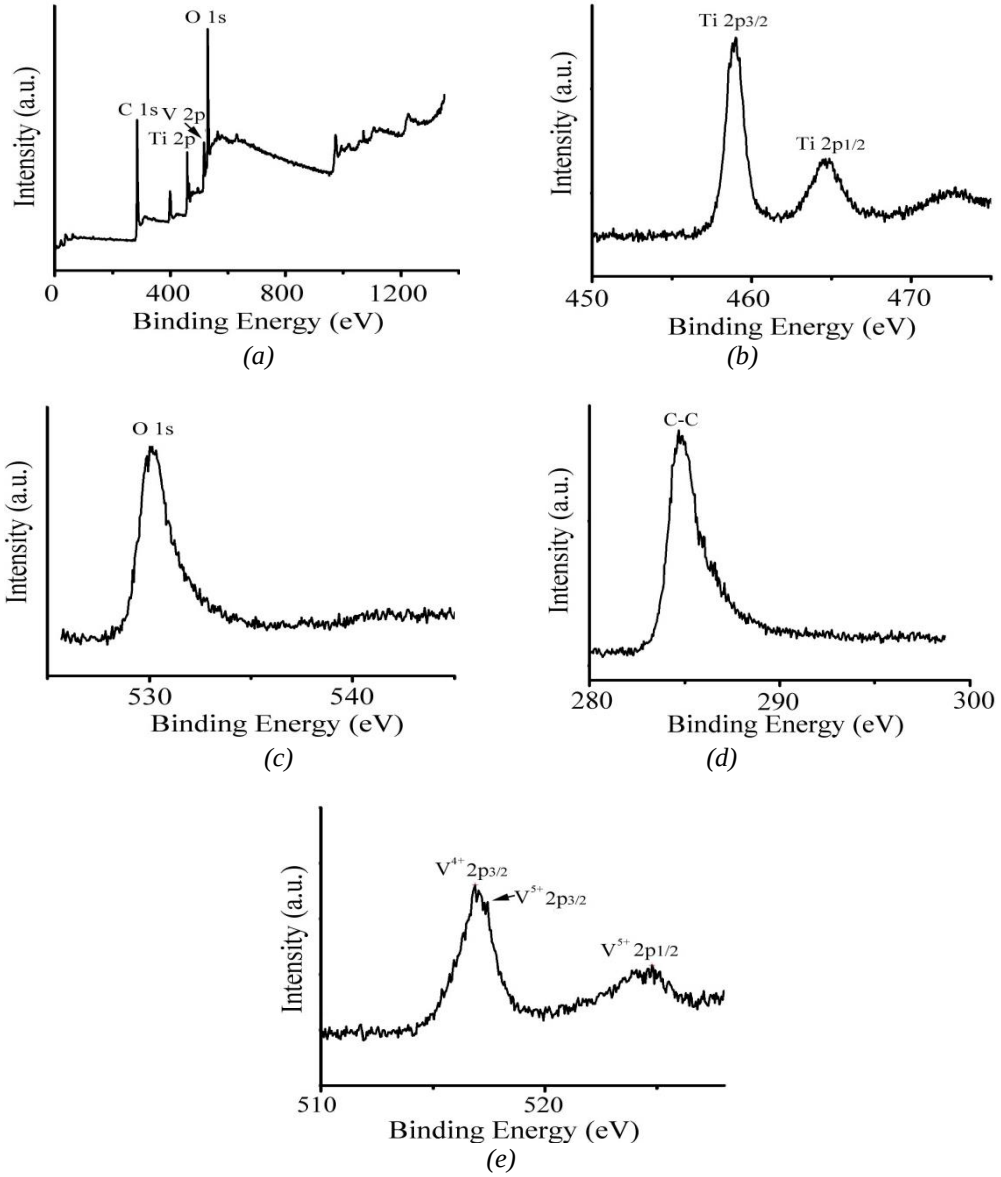

Fig. 4. Typical XPS spectra of the composite: (a) survey spectra, (b) Ti 2p region XPS spectrum, (c) O 2 p region XPS spectrum, (d) C 1s s region XPS spectrum, (e) V 2p region XPS spectrum region XPS spectrum.

The discoloration of MB was used for testing the photocatalytic activities of G/CF, TiO_2, V-TiO_2, and G/CF/V-TiO_2. As seen in Fig. 5, the MB degradation efficiency was in the following order: G/CF/V-TiO_2>V-TiO_2>TiO_2>G/CF. Thus, G/CF/V-TiO_2 showed the best photocatalytic performance under visible light irradiation, wherein it yielded nearly 93.7% reduction in the first 120 min. The reasons for this improvement were attributed to the following factors: (1) the graphene and carbon fiber could act as electron acceptor and promoted the transfer of electrons, thereby preventing the recombination of electron-hole pairs; (2) V-doping could narrow the band gap of TiO_2 and widen the absorption range of TiO_2 to the visible-light region[21].

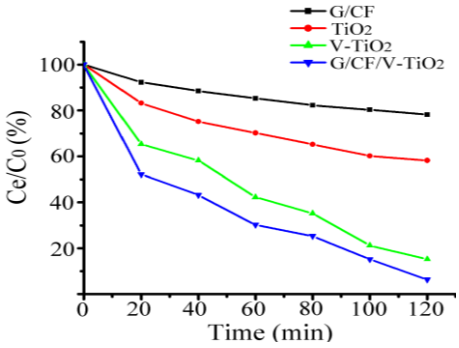

Fig. 5. Photocatalytic degradation efficiency of MB with different catalysts under visible light.

Based on the experimental results, the photocatalytic degradation processes were elucidated as shown in Fig. 6. For pure TiO_2, excitation by visible light did not occur due to its wide bandgap. With doping of V into the TiO_2 lattice a new energy level could be formed by V^{4+}/V^{5+} below the conduction band edge[22]. This resulted in the narrowing of bandgap of TiO_2 and encouraged the significant absorption in the visible light region. Thus, under visible light irradiation, photogenerated electrons were excited to the V^{4+}/V^{5+} energy level, leaving the photogenerated holes at the valence level[22]. With the anchoring of TiO_2 onto the conductive substrate, these photo-generated electrons could easily get transferred onto the surface of the conductive graphene/carbon fibers. This transfer of electrons from the conduction band to the graphene/carbon fibers reduced the recombination of charge carrier at the catalyst[23]. Finally, O_2 accepted the photogenerated-electrons and was reduced to $.O^{2-}$. Both $.O^{2-}$ and holes had strong ability to degrade MB into CO_2 and H_2O[24].

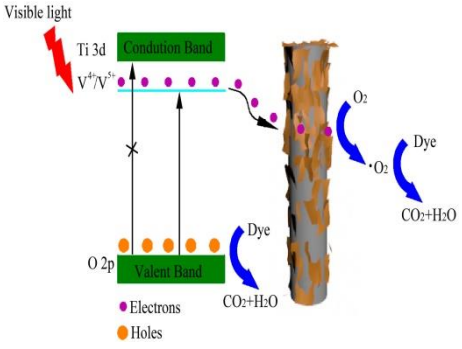

Fig 6. Proposed photocatalytic mechanism of G/CF/V-TiO_2.

4. Conclusions

In summary, graphene and carbon fibers deposited with V-doped TiO_2 nanoparticles were synthesized by electrostatic spinning and carbonization. These composites exhibited excellent photocatalytic activity in the photodegradation of MB under visible light irradiation. The results suggested that graphene/carbon fibers acted as electron acceptor and reduced the recombination of electron-hole pairs. In addition, the V-doped TiO_2 widened the light absorption in the visible light region. Therefore, G/CF/V-TiO_2 materials are expected to be promising candidates for photocatalytic applications.

Acknowledgments

This work was supported by the Project of Hunan Provincial Education Department(19A341) and the project of Hunan Provincial Natural Science Foundation of China (2020JJ6006).

References

[1] X. Y. Liu, C. S. Chen, Mater. Lett. **261**, 127127 (2020).
[2] C. S. Chen, X. Y. Liu, Q. Fang et al., Vacuum **174**, 109198 (2020).
[3] X. H. He, A. Z. Wang, P. Wu et al., Sci. Total Environ. **743**, 140694 (2020).
[4] P. S. Basavarajappa, S. B. Patil, N. Ganganagappa et al., Int. J Hydrogen Energ. **45**, 7764 (2020).
[5] G. Rossi, L. Pasquini, D. Catone et al., Appl. Catal. B-Environ. **237**, 603 (2018).
[6] N. W. Cao, M. Z. Gu, M. M. Gao et al., Appl. Surf. Sci. **530**, 127289 (2020).
[7] M. A. Ashraf, Z. L. Liu, W. X. Peng et al., Ceram. Int. **46**, 7446 (2020).
[8] B. Kakavandi, N. Bahari, R. R. Kalantary et al., Ultrason. Sonochem. **55**, 75 (2019).
[9] M. Li, X. M. Zhang, Y. Liu et al., Appli. Surf. Sci. **440**, 1172 (2018).
[10] Y. Zhang, Z. Shi, L. Luo et al., J Colloid Inter. Sci. **561**, 307 (2020).
[11] A. Sharma, B. K. Lee, Catal. Today **287**, 113 (2017).
[12] C. H. Kim, B. H. Kim, K. S. Yang. Carbon **50**, 2472 (2012).
[13] C. Wang, S. Y. Luo, C. Y. Liu et al., Inorg. Chem. Commun. **115**, 107875 (2020).
[14] S. Y. Cao, T. G. Liu, Y. H. Tsang et al., Appl. Surf. Sci. **382**, 225 (2016).
[15] J. H. Yu, S. H. Nam, J. W. Lee et al., Appl. Surf. Sci. **472**, 46 (2019).
[16] C. A. Aluko, O. Pereao, H. H. Kyaw et al., Mater. Sci. Eng. B **264**, 114913 (2021).
[17] M. S. Stan, M. A. Badea, G. G. Pircalabioru et al., Mater. Sci. Eng. C **94**, 318 (2019).
[18] H. B. Liu, Y. M. Wu, J. L. Zhang, ACS Appl. Mater. Interfaces **3**, 1757 (2011).
[19] Z. G. Li, B. Zeng, Chalcogenide Lett. **18**, 39 (2020).
[20] M. J. Kwon, M. Maniyazagan, H. W. Yang et al., J Alloys and Compd. **842**, 155900 (2020).
[21] I. N. Reddy, L. V. Reddy, N. Jayashree et al., Chemosphere **264**, 128593 (2021).
[22] J. Xu, C. X. Qin, Y. L. Huang et al., Appl. Surf. Sci. **396**, 1403 (2017).
[23] B. Zeng, R. Wang, Dig. J Nanomater. Bio. **15**, 823 (2020).
[24] B. Zeng, W. J. Zeng, Dig. J Nanomater. Bio. **14**, 627 (2019).